BIOPHAM
Bio & Pharmaceutical materials science
EUROPEAN MASTER

UNIVERSITAT POLITÈCNICA DE CATALUNYA
BARCELONATECH

Fitting of complex models of infectious disease with a simple SIRS model.

Name: **Srinivasa Ranganadha Raghavendra Nomula**

Supervisor(s): **Prof. Alonso Muñoz Sergio**

Department and Institution where project was carried out: **DEPARTAMENT DE FÍSICA, UNIVERSITAT POLITECNICA DE CATALUNYA**

Place: **Barcelona, Spain**

Date: 24 **July 2022**

Abstract: Respiratory Syncytial Virus (RSV) significantly impacts children's respiratory health. This study models the spread and impact of RSV using a simplified Susceptible-Infected-Recovered-Susceptible-Reinfected (SIRS'I') model, aiming for comparable results to complex models while maintaining simplicity. Differential equations were solved using Python to simulate population dynamics over 30 years. The model parameters were optimized iteratively. The model also incorporated COVID-like isolation measures and infant vaccination scenarios to study their effects on infected and reinfected populations. The optimized model provided a close fit for the infected population, with COVID-like isolation and vaccination scenarios significantly impacting infection peaks and overall infected population levels.

1. Introduction

Mathematical modelling is a powerful tool for studying the dynamics of transmissible infectious diseases. This report employs mathematical modelling to investigate the dynamics of Respiratory Syncytial Virus (RSV). The modelling approach is based on a modified version of the Susceptible-Infectious-Recovered (SIR) model. The simple SIR model was first introduced by Kermack and McKendrick in 1927 [1], and since then, it has been widely used in modelling the dynamics of infectious diseases.

Respiratory Syncytial Virus (RSV) is a highly contagious virus that causes infections in the respiratory tract. This virus has severe effects on infants less than two years old [2]. However, grown adults are also susceptible to RSV infections [3]. The peak incidence of RSV infection is observed in infants under 12 months [3], after which infected individuals begin to develop immunity against the virus. This immunity is observed to be short-lived, lasting around 200 days [2], making people susceptible to reinfection. Consequently, a notable feature of RSV is its cyclic nature, with severe outbreaks occurring during the winter season and reduced activity in the summer.

The current study involves a modified version of the SIR disease-modelling approach, referred to as the SIRS'I' model. This model is explained using a block diagram in Figure 1, and the corresponding equations are provided in Equations (1) to (5). The SIRS'I' model aims to capture the dynamics of RSV more accurately by including compartments for susceptible (S), infectious (I), recovered (R), re-susceptible (S') and re-infected (I') individuals, reflecting the transient nature of immunity after infection.

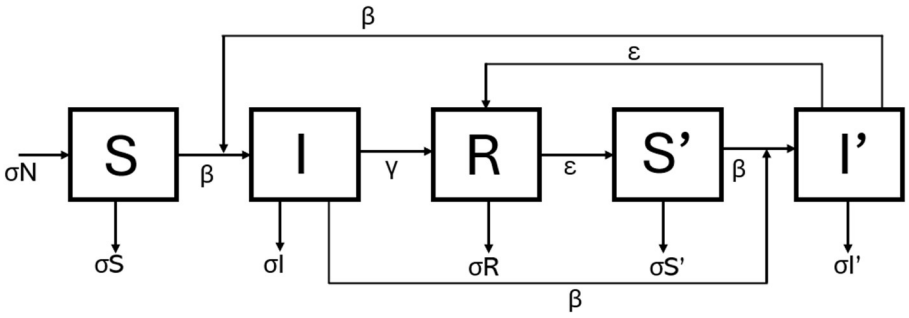

Figure 1. Block diagram for the SIRS'I' ordinary differential equation model

The governing equations for the SIRS'I' model are:

$$\frac{dS}{dt} = -\frac{\beta SI}{N} - \frac{\beta SI'}{N} + \sigma N - \sigma S \quad (1)$$

$$\frac{dI}{dt} = \frac{\beta SI}{N} + \frac{\beta SI'}{N} - \gamma I - \sigma I \quad (2)$$

$$\frac{dR}{dt} = \gamma I + \gamma I' - \epsilon R - \sigma R \quad (3)$$

$$\frac{dS'}{dt} = \epsilon R - \frac{\beta S'I}{N} - \frac{\beta S'I'}{N} - \sigma S' \quad (4)$$

$$\frac{dI'}{dt} = \frac{\beta S'I}{N} + \frac{\beta S'I'}{N} - \gamma I' - \sigma I' \quad (5)$$

$$N = S + I + R + S' + I' \quad (6)$$

Where:

- σ: birth rate = mortality rate
- β: Transmission rate
- γ: Recovery rate
- ε: Rate of losing immunity/ re-susceptible rate
- N: Total population

To keep the model simple and avoid unnecessary complexity, the death rate and birth rate (σ) are kept constant throughout the study. The transmission rate (β) provides information about how many susceptible individuals are getting infected by those with the infectious disease. To account for seasonal behavior, β is considered a cyclic sinusoidal function, represented by the equation (7).

$$\beta = \beta_0 + \delta \cos\left(\frac{2\pi t}{360} + \pi\right) \quad (7)$$

The recovery rate (γ) indicates the amount of time needed for an infected person to completely recover. The parameter (ϵ) represents the rate of loss of immunity in individuals who were infected for the first time and subsequently recovered. This rate, therefore, indicates the rate at which people become re-susceptible to the virus.

The main aim of this study is to develop a mathematical model that is as simple as possible while try to accurately fit the output to that of a more complex model. The equations described above were used to solve ordinary differential equations (ODEs) with Python. The results obtained for a time period of 30 years were then compared with data derived from a more complex model that includes many more parameters.

Further studies were conducted using this simplified model to explore various scenarios. One study included COVID-like isolation measures to examine how quarantine affected the dynamics of disease transmission. Another study investigated the impact of vaccinating different proportions of the population on the dynamics of both infected and re-infected individuals. These additional analyses provide insights into how isolation and vaccination strategies can influence the spread and recurrence of infections.

2. Materials and Methods

This section discusses about the methods used to calculate, optimize and analyse the SIRS'I' mathematical model for population dynamics over a period of 30 years. The model was implemented and solving using Euler's method technique on Python.

2.1. Model description

The mathematical model involves individual compatments for Susceptible(S), Infected(I), Recovered(R), Susceptible again/Re-Susceptible(S' or s) and Reinfected(I' or i).

2.2. Assumptions and Parameters

- The total population size is maintained constant and homogeneous mixing of population is considered.
- Initial conditions: Total population (N) = 7,000,000, Initial infected(I_0) = 307,818, Initial Resusceptible(s_0) = 0, Initial Reinfected(i_0) =31,669 and S_0 = N - I_0 - R_0 - s_0 - i_0 and one year = 360 days
- Parameters: *$\beta(\beta_0$ and $\delta)$, γ, ϵ, σ, and N (total population).*

2.3. Data Sources and implemantation

- Emperical data for all the five compartments were generated from much complex model by Professor Sergio Alonso were provided as .dat files.
- The current mathematical model was solved numerically using Euler's method with a time step(dt) of 1 day over 30 years. Libraries used: 'numpy, 'matplotlib', 'pandas'

- The data of the five compartments generated from the current mathematical model using Python is extraced into Origin 2024b and were plotted against the data from complex model by the professor for comparison.

2.4. Parameter Optimization and Curve fitting:

- To fit the output from the current model,particularly I and i_0, to the data from complex model by optimizing the four parameters β_0, δ, γ *and* ϵ were optimized in two stages.
- Optimization Code 1: β_0 *and* δ are optimized by iterating over a grid of values, calculating the absolute error between current model and empirical(complex) model data, and identifying the absolute minimum error.
- Optimization Code 2: Using the β_0 *and* δ values that yield least absolute minimum error, similar optimisation process is carried out to obtain γ *and* ϵ.
- These two optimization codes were run iteratively, using the improved parameters from each iteration to achieve a close fit between the current model and the complex model.
- Overall error was calculated for the last year which is the 30th year using this formula:

$$\frac{\left|(I_{\text{simulated}} + i_{\text{simulated}}) - (I_{\text{complex}} + i_{\text{complex}})\right|}{360 \text{ days}}$$

- Till here we had employed the same transmission rate β for both susceptible and re-susceptible compartments. To potentially obtain a better fit compared to the previous method, different transmission rates (β for the susceptible population and ηβ for the re-susceptible population) were used. Here, η is a scaling factor used to amplify or reduce the transmission rate for the re-susceptible population

2.5. Simulation of COVID-like Scenario:

- The model was modified to simulate a COVID-like situation by reducing the transmission rate (β) by 50% during specified intervals in the last 5 years of simulated time.
- The impact was analyzed by shifting the 200-day reduction interval by 100 days.

2.6. Vaccination Scenarios:

- The model was further extended to simulate the impact of vaccination starting after 26 years with different vaccination coverage rates.
- In each scenario, different proportions of new borns – 10%, 30%, 50%, 70% and 90% were vaccinated. The dynamics of these vaccination proportions were analzed by comparing the infection dynamics across the different scenarios.

2.7. Code accessibility:

- The Python code and data are accessible via a provided link to a Git hub repository.

3. Results and Discussion

3.1. Parameter Optimization and Curve fitting:

The model parameters are iteratively optimized to minimize the error between the simulated and complex model. Initially a range of β_0 *and* δ values are generated over a grid while keeping γ *and* ϵ fixed. The absolute error between the corresponding simulated values of I and I' and the complex model values for the 30th year was calculated. These error values are plotted in an error grid to visualize the error values over a range of parameter values where green represents the minimum error value and red is maximum. From this grid, the β_0 *and* δ with the minimum error were selected. Using these values, a similar simulation was carried out over a grid of values of γ *and* ϵ values. The γ *and* ϵ with least error were then chosen. This iterative was repeated to achieve the lowest possible error, and the results are shared in the figures : 1, 2, &3 .

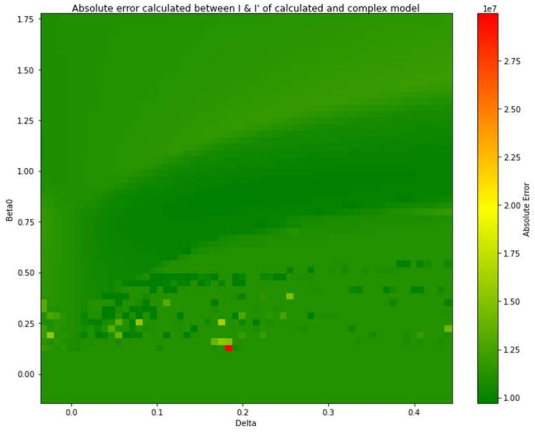

Fig. 1(a)

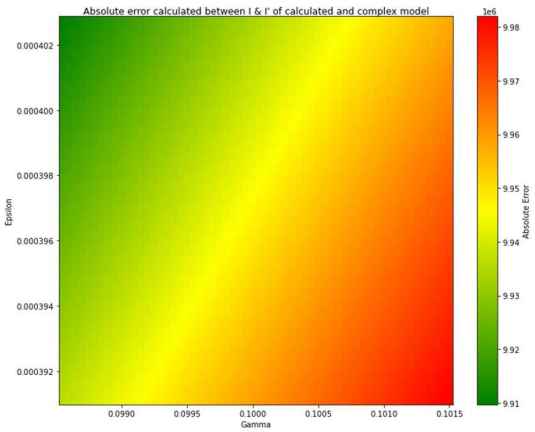

Fig. 1(b)

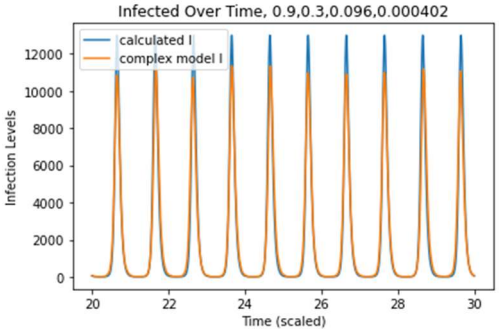

Fig. 1(c)

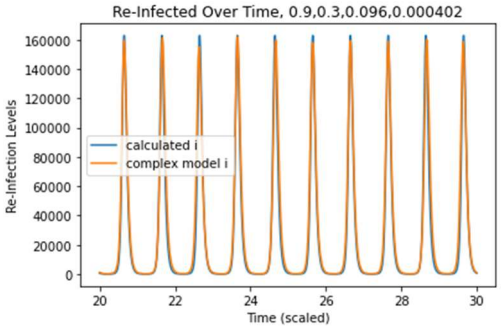

Fig. 1(d)

Figure 1. First simulation (a) Error grid of β_0 and δ from first iteration; (b) Error grid of γ and ϵ using the best parameters from β_0 and δ grid; (c) Infected vs Time(years) in the last 10 years, comparing the values obtained from simulation and those from complex model; (d) Re-infected (I′ or i) vs Time(years) similar to

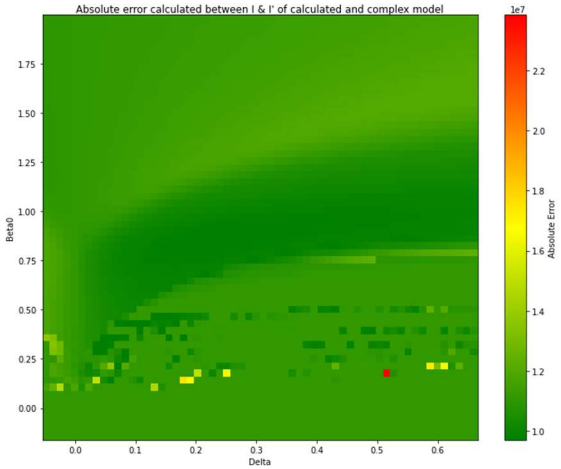

Fig. 2(a)

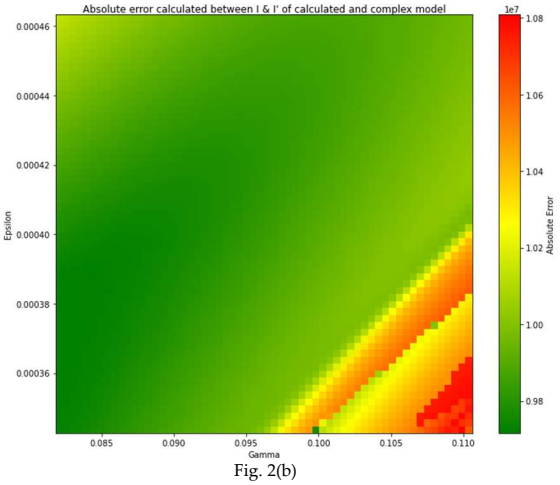

Fig. 2(b)

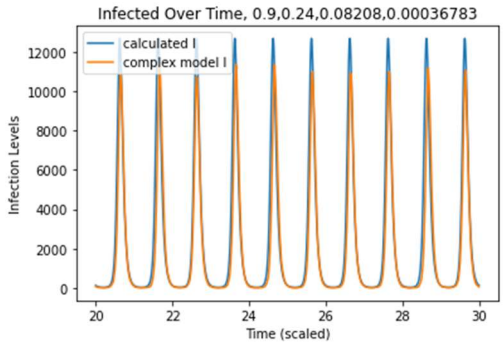

Fig. 2(c)

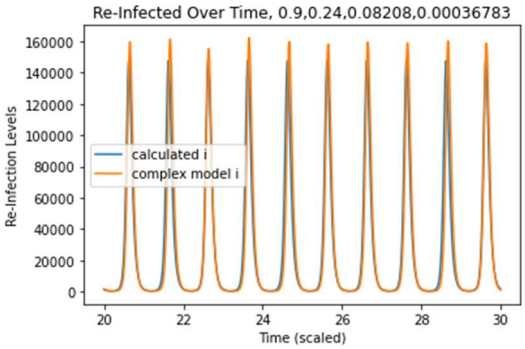

Fig. 2(d)

Figure 2. Second simulation (a) Error grid of β_0 and δ from first iteration; (b) Error grid of γ and ϵ using the best parameters from β_0 and δ grid; (c) Infected vs Time(years) in the last 10 years, comparing the values obtained from simulation and those from complex model; (d) Re-infected (I′ or i) vs Time(years**) similar**

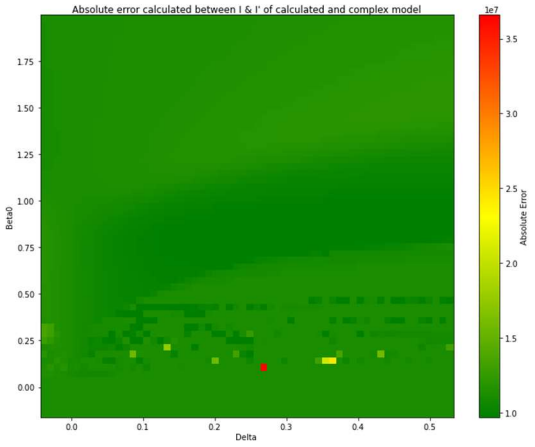

Fig. 3(a)

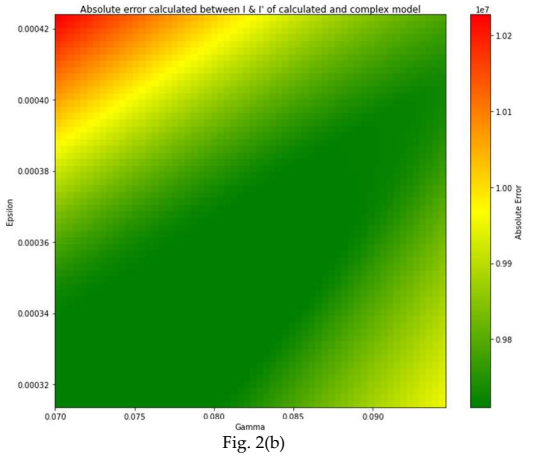

Fig. 2(b)

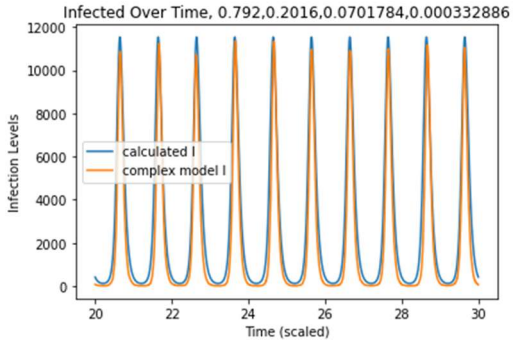

Fig. 3(c)

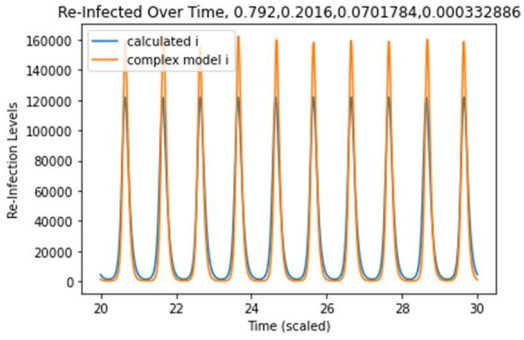

Fig. 3(d)

Figure 3. Third simulation (a) Error grid of β_0 and δ from second iteration; (b) Error grid of γ and ϵ using the best parameters from β_0 and δ grid; (c) Infected vs Time(years) in the last 10 years, comparing the values obtained from simulation and those from complex model; (d) Re-infected (I′ or i) vs Time(years) similar

Table 1. Observations from Three Iterations of Parameter Optimization.

Iteration	β_0	δ	γ	ϵ	Overall error per day for last year
1	0.9	0.3	0.096	0.000402	2730.34
2	0.9	0.24	0.08208	0.00036783	2697.38
3	0.792	0.2016	0.0701784	0.000332886	2697.38

Figures 1(c) and 1(d) illustrate the overlap between the infected and reinfected compartments from the simulated model and the complex model data. In Figure 1(d), a close fit is observed for the reinfected data, whereas in Figure 1(c), the maxima of the infected population each year are higher than those of the complex model. However, the periodicity of both curves remains consistent. In the second iteration, as shown in Figures 2(c) and 2(d), the maxima of both the infected and reinfected populations each year are higher than the corresponding values from the complex model. Despite this, a decrease in the overall daily error is recorded using the parameters from the second iteration compared to the first.

After the third iteration, the parameters obtained result in a close fit between the infected compartments of the simulated and complex data, as observed in Figure 3(c). However, this iteration leads to a lower number of reinfected individuals in the simulation model compared to the complex model each year. The overall daily error remains constant, indicating a trade-off in the current model's ability to fit the data. As the fit for the infected data improves, the fit for the reinfected data worsens. Thus, the parameters from the second and third iterations provided the closest fit between the current SIRS'I' model and the complex model data. Figures 3 to 6 further represent the fit of the remaining compartments of SIRS'I' using the parameters obtained from the three iterations with total population N = 7618000.

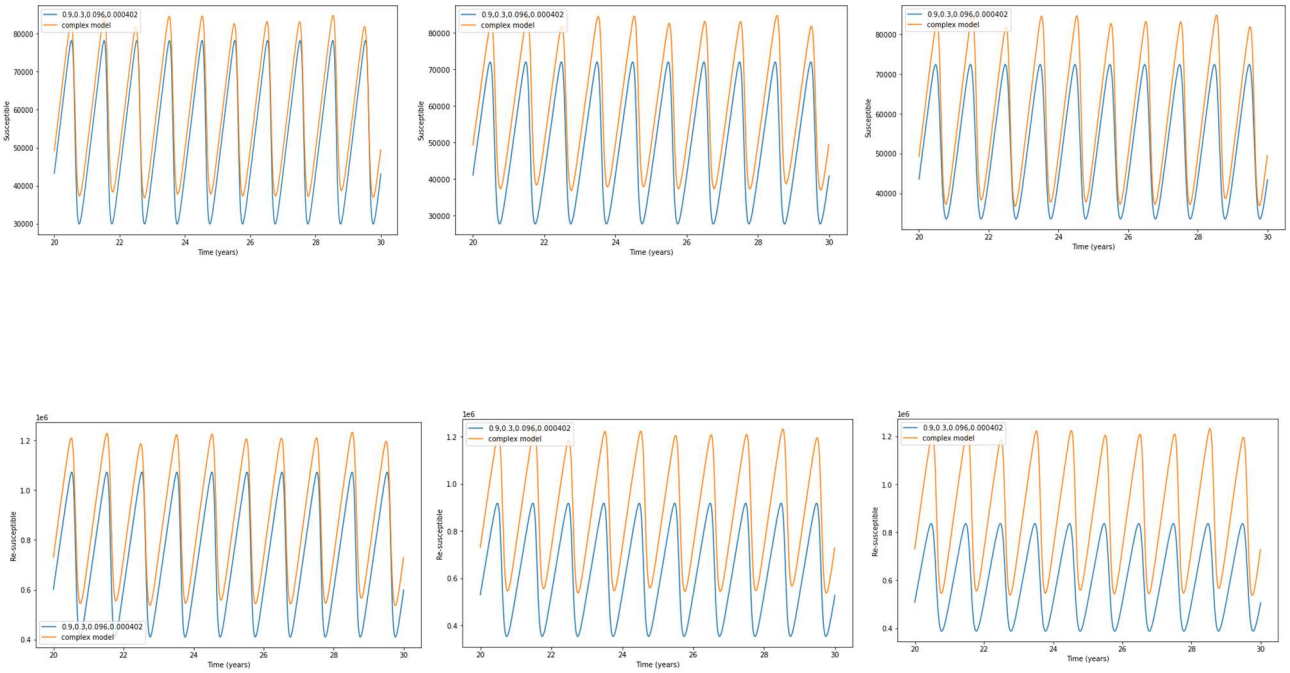

Figure 4. Re-susceptible vs Time(years) in the last 10 years, comparing the values obtained from simulation and those from complex model

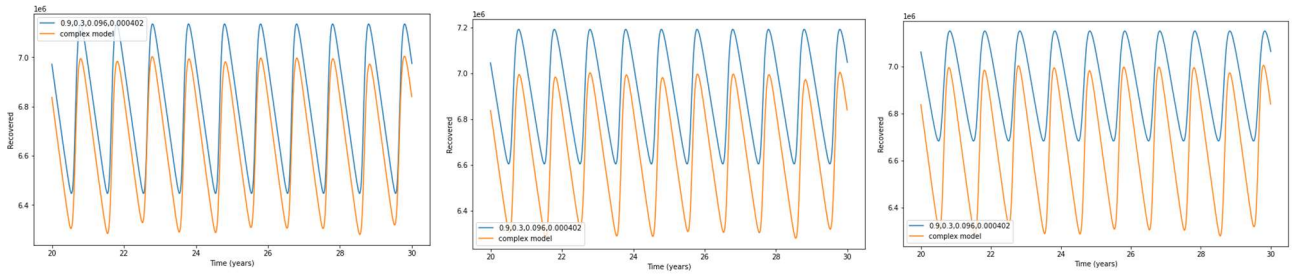

Figure 5. Recovered vs Time(years) in the last 10 years, comparing the values obtained from simulation and those from complex model

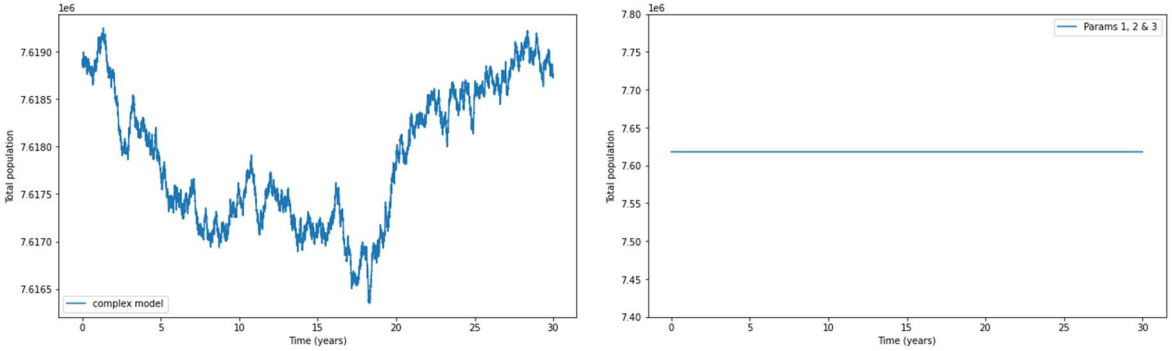

Fig. 6(a) Fig. 6(b)

Figure 6. Total population over years (a) complex model; (b) simulated model

3.1.1 Multiple Transmission Rate:

The effect of different transmission rates on the susceptible (S) and re-susceptible (S') compartments was examined to improve the fit between the simulated and complex models. Various values of the transmission rate scaling factor η were tested, ranging from 0.97 to 1.33.

Despite these adjustments, no significant improvement in the fit of the simulated population to the complex model was observed. However, increasing the η value to 1.33 caused the periodicity of the simulated peaks to shift slightly to the right. Additionally, with higher η values, the difference between the peaks in the reinfected compartment appeared to decrease, but this led to an increase in the overall infected population each year. These observations are illustrated in fig. 7.

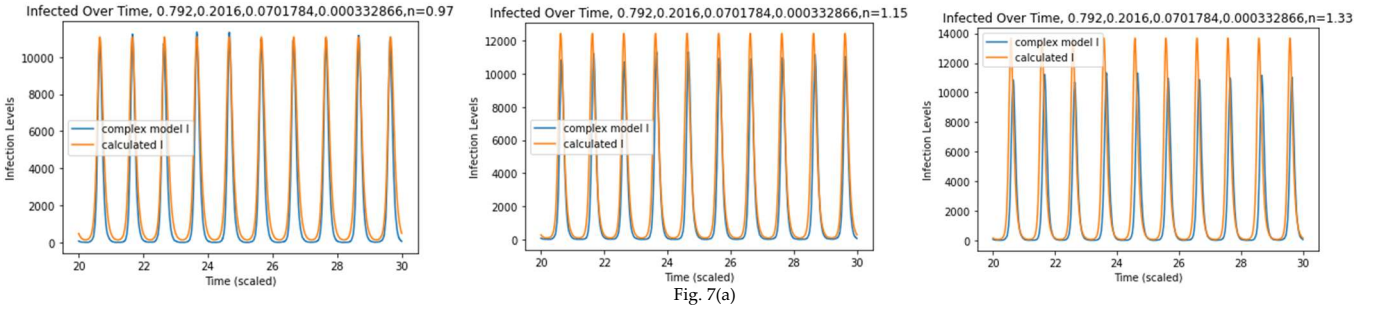

Fig. 7(a)

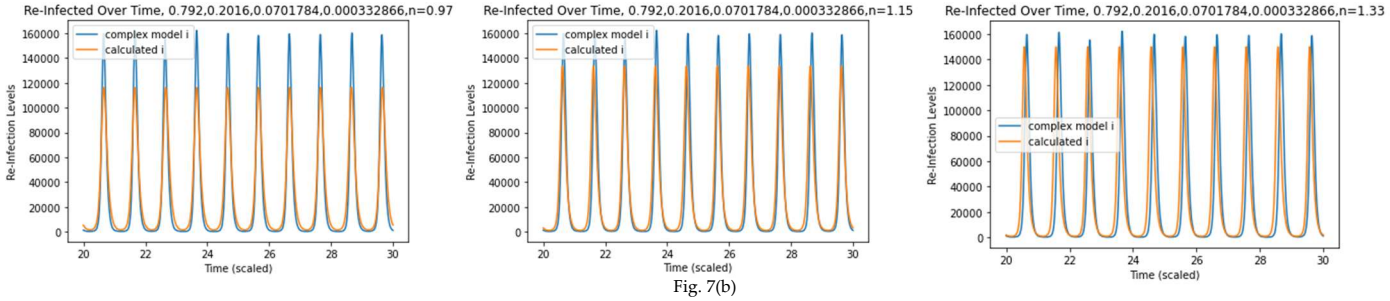

Fig. 7(b)

Figure 7. (a) Infected vs Time(years) in the last 10 years with η = 0.97, 1.15 & 1.33; (b) reinfected vs Time(years) in the last 10 years with η = 0.97, 1.15 & 1.33

3.2. Simulation of COVID-like Scenario:

To further understand the dynamics of the VRS virus, a COVID-like isolation model was implemented. Starting from the 25th year, an isolation period of 200 days was considered, during which the transmission rate was reduced by 50%. After this isolation period, the transmission rate was returned to its original value. The isolation period was then shifted by 100 days, and the study was repeated. This 200-day isolation period was shifted a total of six times to observe the effects of the timing of isolation on the virus dynamics with the parameters from the third iteration.

Additionally, a similar technique was employed with a modified transmission rate reduced by 70% during the isolation period to analyze the impact of a more stringent isolation measure on the population dynamics. Figures 8, 9, 10 &11 show the results of these simulations, comparing the effects of different isolation periods and transmission rate reductions on the infected and reinfected compartments.

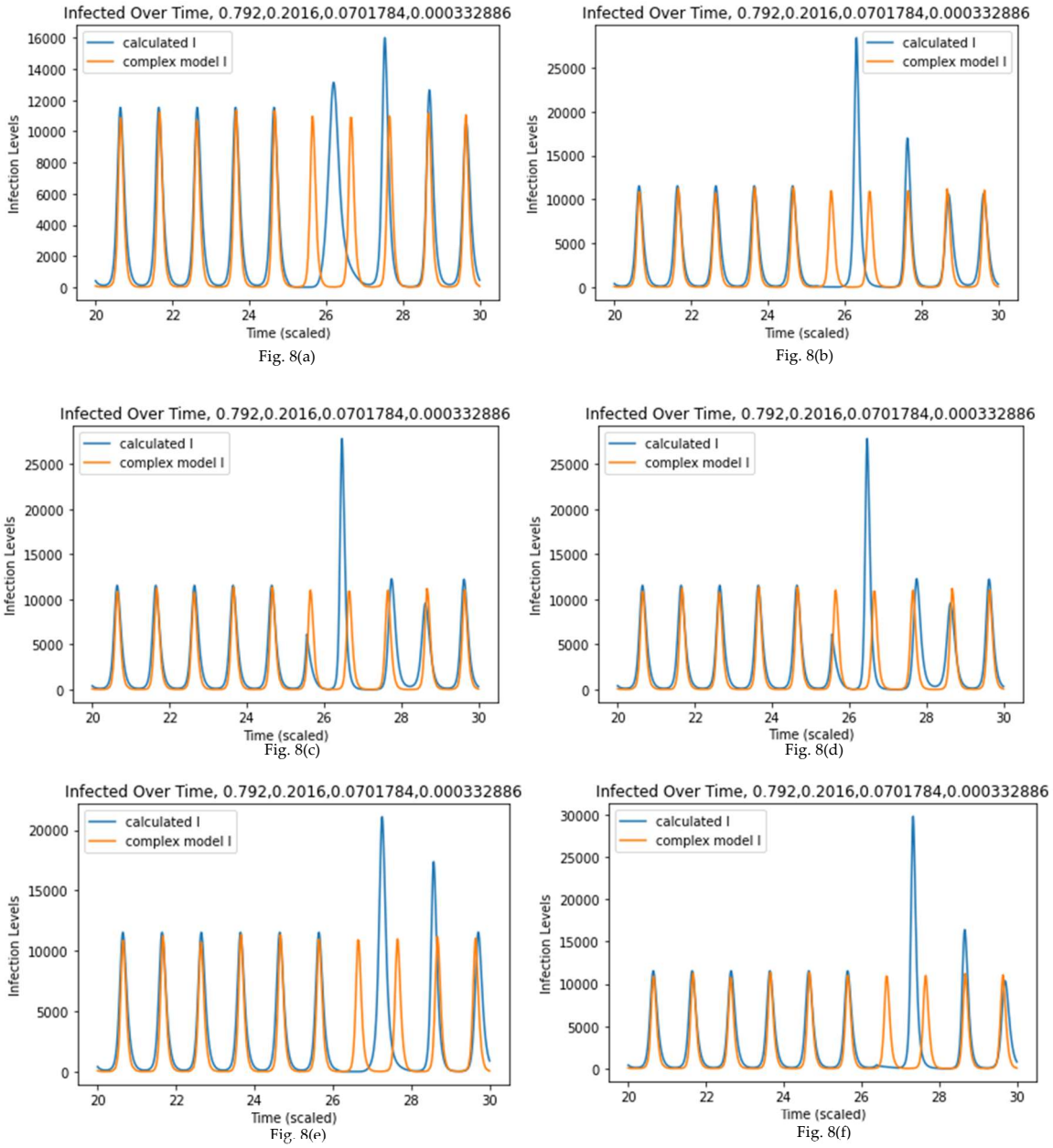

Figure 8. Infected vs Time(years) with 50% reduction in β in the isolation period during (a)9000-9200 days; (b)9100-9300 days; (c) 9200-9400 days; (d) 9300-9500 days; (e) 9400-9600 days & (f) 9500-9700 days.

In the first isolation period, starting from the 9000th day (25th year), Figure 8(a) shows a decline in the infected population during the isolation period. However, immediately after the completion of the 200 days, there is a sharp spike in the total number of infected individuals. At the end of the second isolation period, shown in Figure 8(b), there is an observed increase of more than 100% in the infected population. This second isolation period ends after 300 days in the 25th year, aligning with the winter season, during which the transmission rate (β) reaches its maximum due to its sinusoidal behavior.

Figures 8(c) and 8(d) indicate that the isolation period almost ends in the final months of the winter season, resulting in sharp peaks just after the end of the isolation period. However, the periodicity and maxima of the peaks quickly align with the data from the complex model. In contrast, Figures 8(e) and 8(f), where the isolation period ends after the 26th year 8th month and the 26th year 12th month 10 days respectively, bring the situation back to the winter season, showing dynamics similar to Figure 8(b).

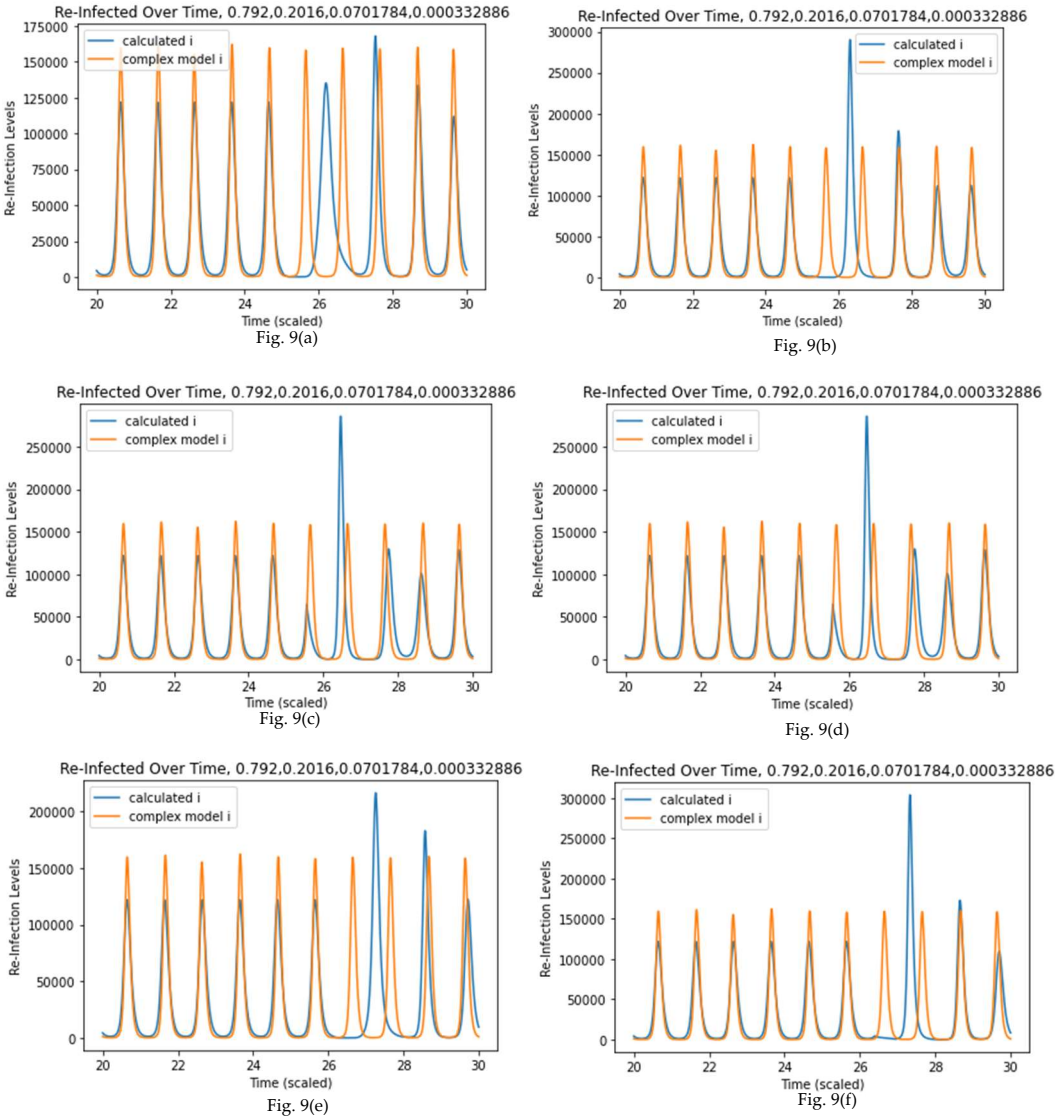

Figure 9. Reinfected vs Time(years) with 50% reduction in β in the isolation period during (a)9000-9200 days; (b)9100-9300 days; (c) 9200-9400 days; (d) 9300-9500 days; (e) 9400-9600 days & (f) 9500-9700 days.

The dynamics of the reinfected population follow similar patterns to the infected population when simulated under the same conditions. These results are visualized in fig. 9. Figures 10 and 11 present a similar study of the COVID isolation model with a 70% reduction in the transmission rate. The isolation period of 200 days with a 100-day shift in each period was simulated three times.

In Figure 10(a), the isolation ends at 9200 days (25th year 7th month). The peak after this period corresponds to an outbreak immediately after the end of the isolation period, caused by the sudden increase in β from 0.3β to β. The subsequent lower-height peak, likely occurring after this initial outbreak, can be attributed to the seasonal reduction in the transmission rate during summer. This seasonal effect, characterized by a naturally lower transmission rate in warmer months, mitigates the spread of the infection, leading to a less pronounced second peak. Following these dynamics, the population in the infected compartment reverted to patterns observed before the isolation period.

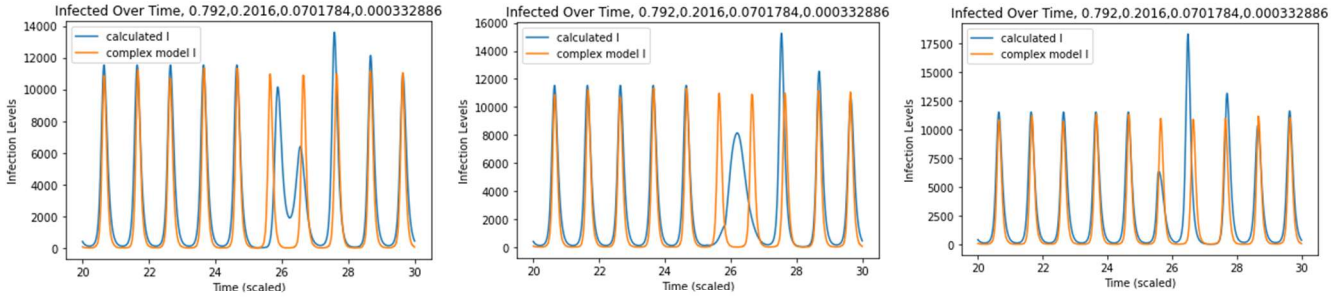

Fig. 10(a) Fig. 10(b) Fig. 10(c)

Figure 10. Infected vs Time(years) with 70% reduction in β in the isolation period during (a)9000-9200 days; (b)9100-9300 days and (c) 9200-9400 days

In Figure 10(b), the isolation period ends in the 25th year 10th month, and in Figure 10(c), the isolation period ends after 26 years 2 months and 10 days. The transition from the reduced transmission rate back to the higher value may take some time for the population to build up the infection, resulting in a transition phase. The first peak after the isolation period in Figure 10(c) ends around the end of the winter season. Therefore, β is lower compared to the case in Figure 9(b), resulting in a lower peak during the transition phase. This is followed by the infection dynamics converging to patterns similar to those observed before the isolation period. The dynamics of the reinfected population follow similar patterns to the infected population when simulated under the same conditions. These results are visualized in fig. 11

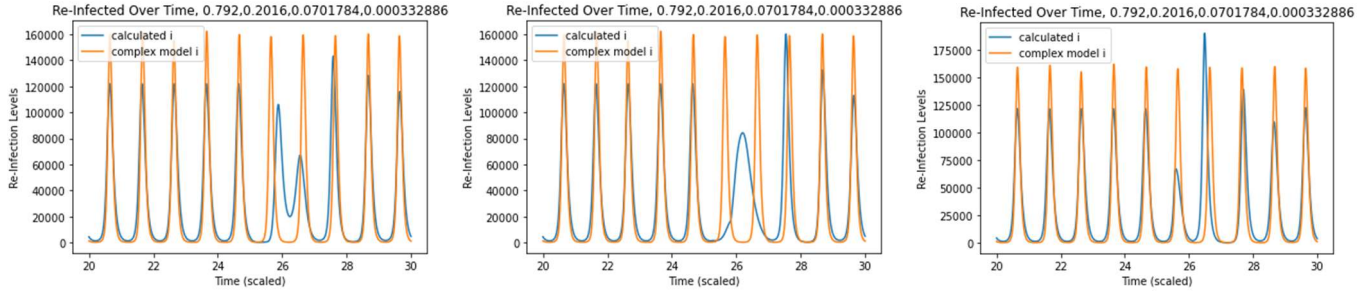

Figure 11. Reinfected vs Time(years) with 70% reduction in β in the isolation period during (a)9000-9200 days; (b)9100-9300 days; (c) 9200-9400 days; (d) 9300-9500 days; (e) 9400-9600 days & (f) 9500-9700 days.

3.3. Vaccination Scenarios:

Following the COVID-like scenario, the mathematical model was further modified to include vaccination of infants in order to study its impact on population dynamics, particularly in the infected and reinfected compartments. The effects of vaccination are visualized in the accompanying figures.

Different proportions of newborns were vaccinated, including 10%, 30%, 50%, 70%, and 90% from the 26th year onward. As the percentage of vaccinated newborns increased from 10% to 90%, there was a significant reduction in the overall infected population, with the maximum number of infected individuals converging to a lower peak value. A major decrease in the number of infected individuals was observed as vaccination rates increased from 50% to 90%, as depicted in the fig. 12 (a) to (e).

However, the impact of vaccination on the reinfected population was less pronounced, particularly at the 10% and 30% vaccination levels. A significant decrease in the reinfected peak, by approximately 10,000 individuals, was observed at the 70% and 90% vaccination levels. These results highlight the importance of high vaccination coverage in controlling the spread of the infection and reducing the number of reinfected individuals, as depicted in the fid. 13 (a) to (e).

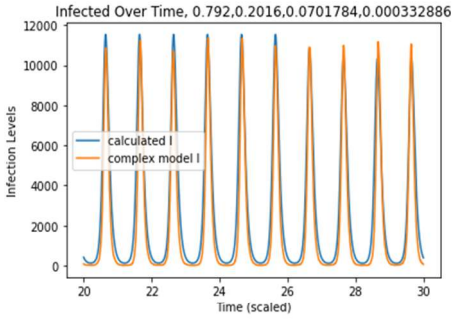

Fig. 12(a)

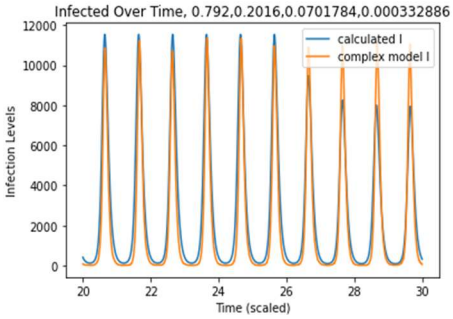

Fig. 12(b)

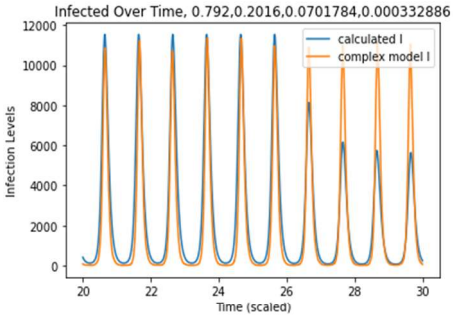

Fig. 12(c)

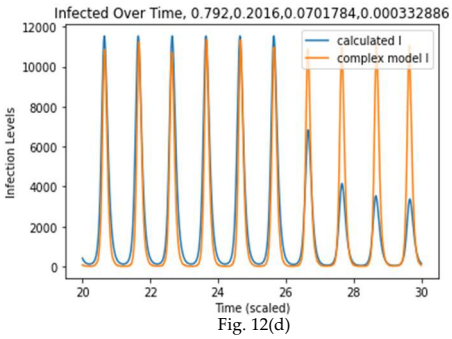

Fig. 12(d)

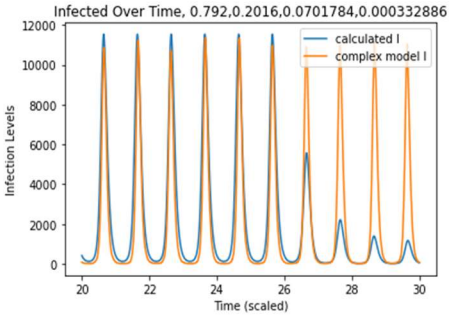

Fig. 12(e)

Figure 12. Infected vs Time(years) with vaccination of (a) 10%; (b) 30%; (c) 50%; (d) 70% & (e) 90% the infant population.

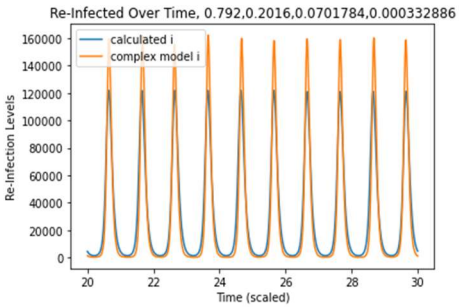

Fig. 13(a)

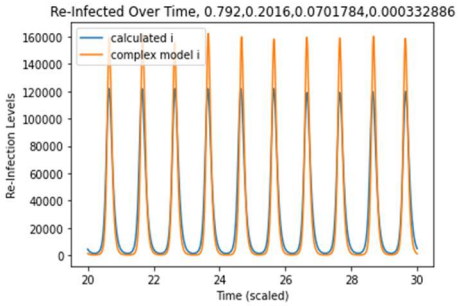

Fig. 13(b)

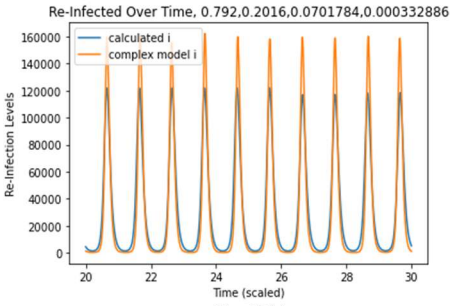

Fig. 13(c)

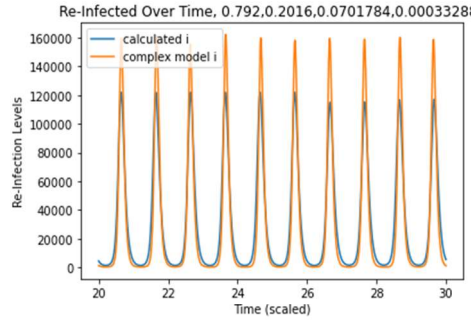

Fig. 13(d)

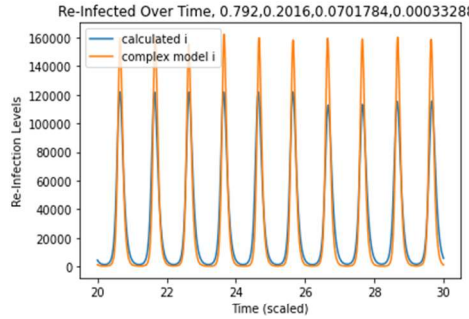

Fig. 13(e)

Figure 13. Reinfected vs Time(years) with vaccination of (a) 10%; (b) 30%; (c) 50%; (d) 70% & (e) 90% the infant population.

4. Conclusions:

The model parameters were iteratively optimized to minimize the error between the simulated and complex model outputs. The final parameters obtained in the second iteration and third iteration provided a close fit for the infected population but showed a trade-off in fitting the reinfected population. The introduction of COVID-like isolation periods showed significant impacts on infection peaks, with the timing of the isolation playing a crucial role in infection dynamics. Vaccination scenarios demonstrated that higher vaccination coverage significantly reduces the overall infected population, with notable improvements observed at 70% and 90% coverage rates. This study demonstrates that a simplified SIRS'I' model can effectively simulate the dynamics of RSV infections and yield results comparable to

complex models. Also, these findings highlight the importance of vaccination coverage in controlling the spread of infections and suggest that the timing of isolation measures is critical in managing outbreaks. Future research could explore further parameter optimizations for better fit and to enhance model accuracy.

References

1. Kermack, W.O., McKendrick, A.G.: A contribution to the mathematical theory of epidemics. Proc. R. Soc. Lond, **1927,** A. 115, 700–721
2. Weber, A.; Weber, M.; Milligan, P. Modeling epidemics caused by respiratory syncytial virus (RSV). Math. Biosci. **2001**, 172, 95-113.
3. Hogan, A.B., Glass, K., Moore, H.C., Anderssen, R.S. Age Structures in Mathematical Models for Infectious Diseases, with a Case Study of Respiratory Syncytial Virus. In *Applications + Practical Conceptualization + Mathematics = fruitful Innovation*, 1st ed.; Anderssen, R.S., Broadbridge, P., Fukumoto, Y., Kajiwara, K., Takagi, T., Verbitskiy, E., Wakayama, M., Eds.; Springer: Tokyo, Japan, 2016; Volume 11, pp. 105-116.